CLIMATIC IMPORTANCE OF THE MODULATION OF THE 100-KYR CYCLE INFERRED FROM 16-MY LONG MIOCENE RECORDS

L. Beaufort

PALEOCEANOGRAPHY, VOL. 9, NO. 6, PAGES 821-834, DECEMBER 1994

Climatic importance of the modulation of the 100 kyr cycle inferred from 16 m.y. long Miocene records

Luc Beaufort

Laboratoire de Géologie du Quaternaire, CNRS-Luminy, Marseille, France

Abstract. The variations of the amplitude of the 100 kyr cycle are not yet clearly understood. Although the timing of the appearance of these cycles in the Pleistocene is well established, very little is known about the occurrence of such cycles and their evolution in most of the Neogene. Two detailed and continuous 16 m.y. long Miocene records of paleoceanographic significance are analyzed in order to study the dynamics of the 100 kyr cycle. One record results from counts of the relative abundance of the calcareous nannoplankton *Coccolithus pelagicus* in about 1000 samples taken in the Neogene section recovered from Ocean Drilling Program site 747 (southern Indian Ocean). This record, in which the chronologic resolution is ~17 kyr, is interpreted as reflecting migrations of the Antarctic polar front through time. The record of the wet-bulk density in the same section, which is interpreted as reflecting variations of paleoproductivity constitutes the second 16 m.y. record. It has a chronologic resolution of 3.5 kyr. The two series reveal the presence of 100 kyr cycle during the Miocene. This cycle is not stable through time and vary similarly in the two series. The amplitude of the 100 kyr cycle fluctuates quasi-periodically with primary periods close to 2.38, 1.14, and 0.8 m.y., equivalent to those of the modulation of the orbital parameters (obliquity and eccentricity). In addition, the amplitude of the 100 kyr cycle is stronger during cooler times. The interactions between climate and modulation of the eccentricity or the obliquity cycles are good candidates to explain that change in amplitude. It is concluded that the long term modulation of the orbital parameter has a significant influence on global climate.

Introduction

In the astronomical theory of climate the 100 kyr cycle (all cycles in the frequency band comprised between 90 and 140 kyr, usually related to the eccentricity system) occupies the most intriguing place. Although it is the dominant cycle recorded by late pleistocene paleoclimatic proxies [*Hays et al.*, 1976a], it is difficult to explain it in terms of a direct response to the forcing of the eccentricity. It has been ascribed to nonlinear feedbacks resulting from different time constants of the decay and growth of ice sheets [*Imbrie and Imbrie*, 1980], as well as ice sheet/bedrock dynamics [*Oelermans*, 1980; *Pollard*, 1983], to interaction of different components of the climate system [*Saltzman*, 1987] and to asymmetry of the obliquity cycles [*Liu*, 1992]. *Imbrie et al.* [1993] review most of the possible causes of the presence of the 100 kyr cycle in the Pleistocene and identify massive northern hemisphere ice sheets as responsible of that prominent response of the Earth climate in this frequency band. Most intriguing is the fact that the 100 kyr cycle is not stable through time: it is recorded for the past 0.75 m.y. but not between 0.75 and 1.25 Ma [*Pisias and Moore*, 1981; *Ruddiman et al.*, 1986, 1989]; it is expressed in series between 1.6 and 2.1 Ma [*Raymo et al.*, 1989] and between 4.9 and 5.75 Ma [*Beaufort and Aubry*, 1990] but not between 2.1 and 2.75 Ma [*Raymo et al.*, 1989] and between 5.75 and 6.3 Ma [*Beaufort and Aubry*, 1990]. *Park and Maasch* [1993] found evidence that it did not disappear truly from 1.25 to 0.75 Ma but was instead of lower amplitude than during the late Pleistocene. The 100 kyr cycle had also been found in various records from presumably nonglacial periods like the Cretaceous [e.g., *Herbert and Fischer*, 1986]. The question of why its amplitude varied through time remains unsolved. The appearance of this cycle in the late Pleistocene has been ascribed to the large increase in ice volume related to atmospheric CO_2 decrease by *Saltzman and Verbitsky*

Paper number 94PA02115.
0883-8305/94/94PA-02115$10.00

[1992] and to late Neogene uplift in Asia and America by *Raymo et al.* [1989] and by *Ruddiman and Raymo* [1988]. Neither mechanism can, however, explain the apparently episodic appearance of the 100 kyr cycle.

In order to understand how the amplitude of this cycle has varied through time, it is necessary to establish a precise history of their variations through the study of several million years continuous records. In this study I analyze two detailed 16 m.y. long records (one paleontologic and one sedimentologic) of paleoceanographic significance, which serve to describe for the first time the modulation (variation of the amplitude) of the 100 kyr cycle over a long period of time.

Setting and Material

The thick Neogene section recovered from Ocean Drilling Program site 747 on Kerguelen Plateau (southern Indian Ocean) (Figure 1) offers the rare qualities (continuity and highly detailed chronology) required for long time series analysis. A precise chronologic framework for most of the Miocene section was obtained through the integration of an excellent paleomagnetic record [*Heider et al.*, 1992] with biostratigraphic data (foraminifera, diatoms, and radiolarians) [*Schlich et al.*, 1989]. The most recent age estimates of the magnetic reversals by *Cande and Kent* [1992] are used here in order to update the chronology. This continuous 16 m.y. sequence spans the interval between 8.8 Ma (Chron C4A) and 24.7 Ma (Chron C7) with a remarkably constant sedimentation rate of about 5 m/m.y. (Figure 2). The diversity of the calcareous nannofossil assemblages is extremely low. *Coccolithus pelagicus*, and a few species belonging to the genus *Reticulofenestra* (*R. minutula, R. pseudoumbilica, R. floridana*, and *R. perplexa*) represent more than 98% of the Miocene assemblages. The first record corresponds to the counts made by *Beaufort and Aubry* [1992] of the ratio between *C. pelagicus* and the rest of the assemblages in 936 samples taken at 10 cm sampling interval corresponding to a chronologic resolution of about 17 kyr (Figure 3). The second is the record of the wet bulk density determined by the gamma ray attenuation porosity evaluator (GRAPE), which was measured during leg 120 [*Schlich et al.*, 1992] at a sample spacing of 2 cm corresponding to a chronologic resolution of 3.4 kyr (Figure 3). ODP site 747 was not doubled HPC, and it is not possible to make a composite depth scale for these cores. The gap between the nine cores studied here cannot be estimated. Any gaps are interpreted to be relatively small because of the linearity of the sedimentation rate (Figure 2).

Statistical Technics

The statistical techniques used in this paper are standard procedures based on the Fourier transform, which permits an estimation of the power density spectrum of

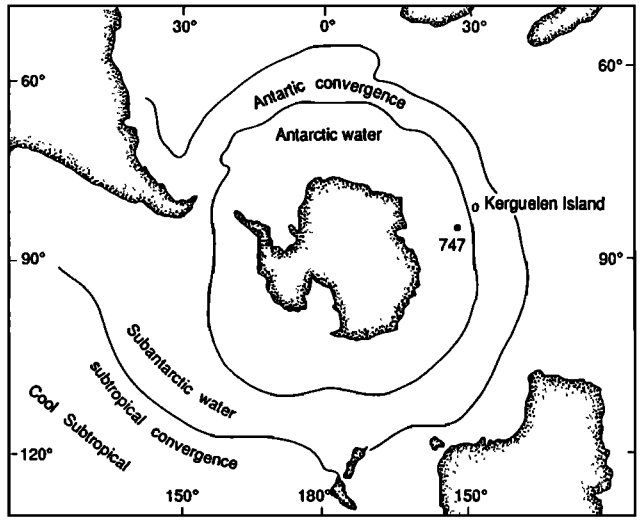

Figure 1. Location of Ocean Drilling Program site 747. The polar front (or Antarctic convergence) is a pronounced feature of the Antarctic Ocean, located North of the site. This modern type of circumpolar circulation around Antarctica began prior the Miocene [e.g., *Wright et al.* 1992a] but the position of the front fluctuated latitudinally in response to climatic variations [e.g.: *Hays et al.*, 1976b].

series, the coherency and phase between two series, and filtering of the series at given frequencies (band pass filtering). The programs used belong to a package written by D. Paillard (CFR, Gif/Yvette, France) in a large part inspired from routines of SPECMAP programs and Numerical Recipes [*Press et al.*, 1986]. Spectral estimates of these records are made using both Blackman-Tukey and maximum entropy algorithms [e.g., *Jenkins and Watts*,

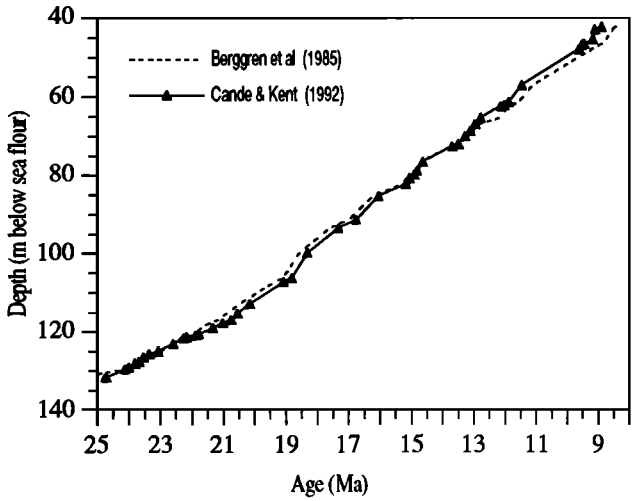

Figure 2. Sedimentation rate curve at ODP site 747. The triangles represent the magnetic reversals [*Heider et al., 1992*]. The magnetochronology is that of *Cande and Kent* [1992] (solid line); for comparison, the sedimentation rate curve based on the magnetochronology of *Berggren et al.* [1985] is given (dotted line).

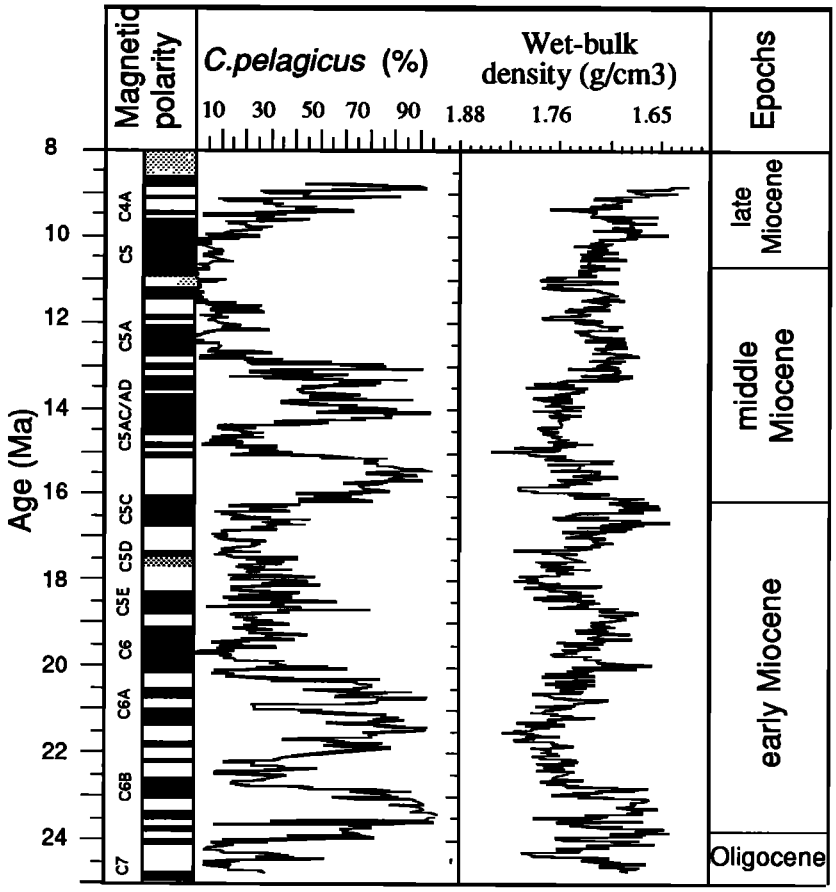

Figure 3. (Left) Relative abundance (%) of *Coccolithus pelagicus* in Miocene sediments at ODP site 747, estimated from the counts of more than 200 specimens in each of the 936 samples. (Right) Wet-bulk density measured by GRAPE [*Schlich et al.*, 1989]. To be readable the curve was smoothed with a ten point running average (the original data set had been used elsewhere in this study).(Left column) Magnetic polarity log from site 747 [*Heider et al.*, 1992] (shaded areas indicate noninterpretable data).

1968, *Press et al.*, 1986]. The maximum entropy method gives very high resolution spectra which help to precisely estimate frequencies peaks. With this latter method, however, there is no test for evaluating the significance of the peaks. Also, an abundance of spurious peaks may be found when too high an order of resolution is chosen [*Press et al.*, 1986]. These authors recommend the use of this algorithm in conjunction with more conservative methods. The Blackman-Tukey technique is used for this purpose with the maximum entropy because it is usually considered statistically robust, allowing an estimation of the significance of peaks; it is often used by paleoclimatologists. The phases and coherencies between series are calculated by Cross-Blackman-Tukey.

A large part of the analysis is also based on band-pass filtering. The method consists of a convolution with a Gaussian window. Usually, the two ends of the filtered series are lost but by using a cyclic convolution it is possible to recover these lost parts and to present them in the figures; however, because of uncertainty, the recovered parts are not used further in spectral analysis. For comparison, other programs and filtering technics have been used on paleoceanographic time series (recursive filtering and program of SPECMAP). They produce very similar results.

The envelopes of the filtered series have been derived by connecting the absolute values of the maxima (upper envelope) and the minima (lower envelope) of the band-pass filtered records. The results obtained with the Hilbert transform were compared with those obtained by connecting of maxima and minima. The two methodologies for calculating the envelope produce analogous results.

Significance of the Selected Records

The *Coccolithus pelagicus* record is interpreted in terms of water mass movements. The cold water species *C. pelagicus* [*McIntyre*, 1967; *Braarud*, 1979; *Haq*, 1980] was the dominant species in water located south of a front regarded as a Miocene equivalent of the present polar front (Figure 1), whereas *Reticulofenestra pseudoumbilica* and other related species, which seem to be ecologically less

sensitive [*Haq*, 1980], dominated the more temperate northern waters. Fluctuations in the percentage of *C. pelagicus* at ODP site 747 (Figure 3) reflect movements of the southern water mass over this site as well as over nearby ODP sites 751 and 748, located 300 to 400 km to the south, sites where the abundance increases in *C. pelagicus* happened slightly before those at site 747 and with a stronger amplitude [*Beaufort*, 1992 also unpublished data]. Pleistocene polar front movements in the Antarctic Ocean were linked to climatic variations and indirectly to Antarctic ice volume, and migrations of this front have been recorded between glacial and interglacial stages (reaching 7° in latitude) [e.g., *Hays et al.*, 1976b; *Howard and Prell*, 1992].

The wet-bulk density is closely related to the carbonate content of pelagic sediments and reflects differences in packing between carbonate and non-carbonate particles [*Herbert and Mayer*, 1991]. A good correlation was found between dry- and wet-bulk density and carbonate content in sediment from the nearby ODP site 751 [*Howard*, 1992; *Rack and Palmer-Julson*, 1992]. The variations in carbonate percent in leg 120 sediments (and hence physical properties fluctuations) reflect changing carbonate productivity and dilution by biogenic silica [*Howard*, 1992; *Rack and Palmer-Julson*, 1992], the sediment being composed primarily of calcareous nannofossils and diatoms. Carbonate variations at site 747 cannot result from dissolution because this site was drilled by 1695 m of water depth well above the lysocline and also because the coccoliths do not present any trace of dissolution. Because the diatoms are known to prefer nutrient-rich waters in contrast to the calcareous nannoplankton, the site 747 wet-bulk density record represents a proxy of paleofertility. Relations between oceanic productivity and climate in the vicinity of site 747 during the Miocene exist but are complex because changes in oceanic productivity reflect changes in global productivity as well as changes in ocean circulation, but also local movements of water masses in the vicinity of a convergence zone [*Beaufort*, 1992]. The intricate climatic meaning of this record is problematic but because of its higher temporal resolution, it can serve for the validation of spectral characteristics found in the *C. pelagicus* record, especially concerning sample aliasing.

The 100 Kyr Cycle

Spectral analysis of both records (both Blackman-Tukey and maximum entropy were used) shows significant power rising at periods which closely correspond to the major terms of the eccentricity cycles (95, 124, 404 kyr) [*Berger and Loutre*, 1991] (Figure 4 and 5). As the chronologic resolution in the wet-bulk density record is 3.4 kyr (which is far from 20 kyr), the 100 kyr cycle found in the series cannot result from sample aliasing [*Jenkins and Watts*, 1968] in the precession frequency band. These results are robust and not dependent on the chronological model used: the same periods were found using the *Berggren et al.* [1985] time scale [*Beaufort and Aubry*, 1992] (which differs by about 5% from the magnetochronology of *Cande and Kent* [1992] used here; see Figure 2). Finally these cycles are stable and are found in different parts of the series. The same frequencies occur between 16.2 and 20 Ma, which is the longest stable interval of the *C. pelagicus* record (i.e., where no long-term variations affect the spectral analysis) (Figure 6), but also in other intervals [*Beaufort and Aubry*, 1992]. The periodogram (Figure 6) shows the presence of significant peaks at 122 and 94.7 kyr which are equal to the predicted eccentricity cycles (123.8 and 94.7 kyr).

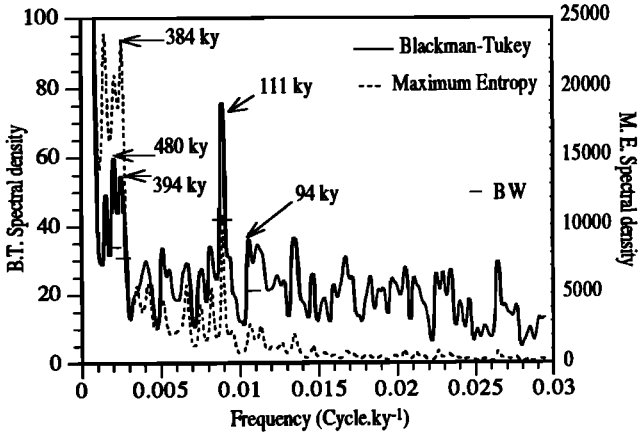

Figure 4. Periodograms of the entire series of abundance in *C. pelagicus* (series shown in Figure 2). (Solid line) Blackman-Tukey spectral analysis with a prewhitening of 0.6. (Dashed line) Maximum entropy spectrum (without prewhitening). These two independent methods of spectral analysis reveal the same periods which enhance confidence in the analysis. BW is bandwidth, and small horizontal bars within peaks are the lower bounds of one-sided 95 % confidence intervals attached to estimates of peak heights.

The wet-bulk density record is sampled finely enough (3.5 kyr) to test the presence of the precession and the obliquity cycles in the series. However, in our series these cycles have an average depth length of about 10 and 20

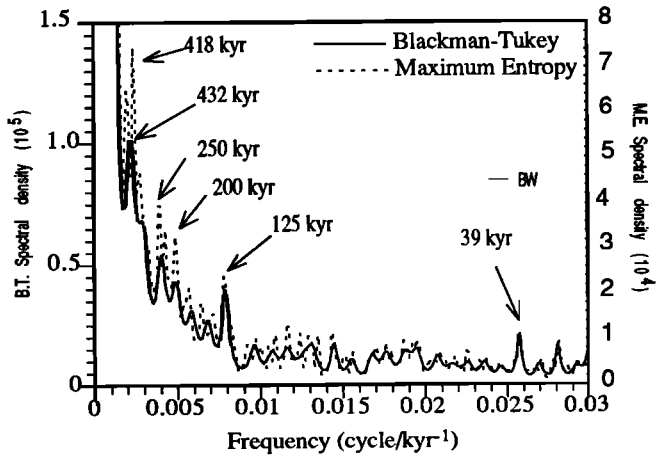

Figure 5. Periodograms of the wet-bulk density series. (Solid line) Blackman-Tukey spectral analysis. (Dashed Line) Maximum entropy spectrum.

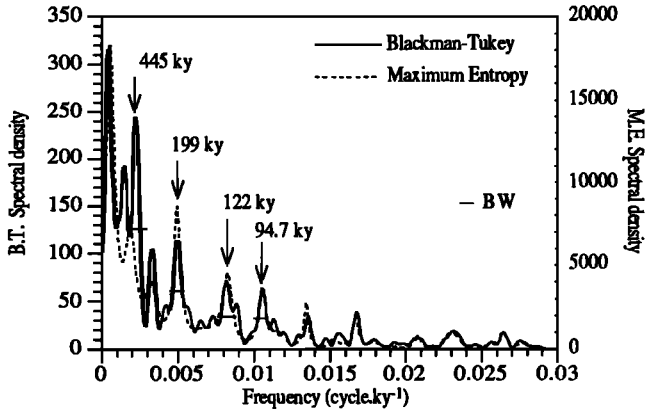

Figure 6. Periodograms of the longest stationary part of the coccolith series (16.2 to 20 Ma). Same characteristics than in Figure 4 but Blackman-Tukey without prewithening. Note the presence of a double peak around 100 kyr (at 94.7 and 122 kyr. (Equivalent periodograms (not shown) were obtained using other parts of the record with a lower accuracy because of shorter subseries. In rare cases no eccentricity cycles were found).

cm. Bioturbation and/or small variations of the sedimentation rate greatly alter the sharpness and the resolution of the record of these cycles in the site 747 series. Consequently, the peaks in the periodograms in the high-frequencies band (obliquity and precession) are extremely weak. For the entire density series a Blackman-Tukey had been computed with a limited number of lag (1%) in order to limit the number of spectral estimates in the high frequency band. The results (Figure 7) show significant power at 23 and 18 kyr corresponding to

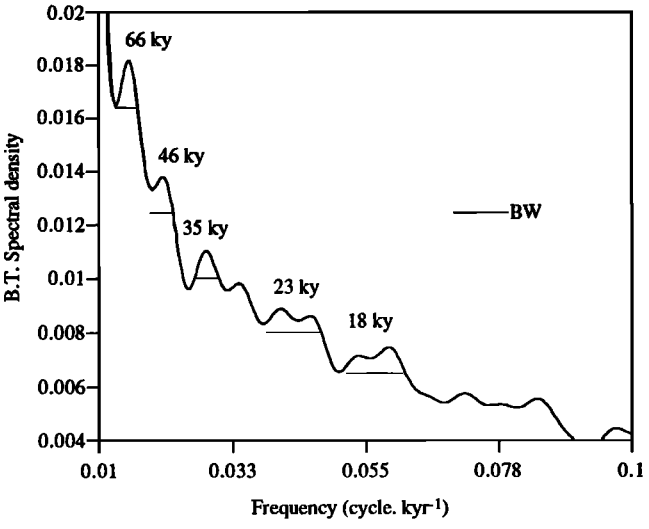

Figure 7. Periodogram (Blackman-Tukey) of the wet-bulk density record with a reduced number of lags (1% of the series) in order to give a good confidence in the high frequency domain with a sufficient resolution to solve the existence of precession and obliquity signal. Two peaks at 23 and 18 kyr are interpreted to be those of the precession.

precession cycles. The series is filtered with a band-pass filter centred on 1/20 kyr^{-1}, with cutting frequencies of 1/17 and 1/24 kyr^{-1}. A spectral analysis of the envelope is then computed which reveal the presence of strong 128 and 114 kyr peaks (Figure 8), which corresponds to the 125 kyr cycle found in the raw data (Figure 5). This observation correspond to the fact that the eccentricity cycles modulate the precession cycles [e.g., *Imbrie et al.*, 1993, Figure 8], and in consequence validate an orbital imprint in the density series. Also, the increases of the amplitude of the precession follow those of the eccentricity as in the Pleistocene [e.g., *Park and Maasch*, 1993, Figures 11 and 12].

In order to characterize the amplitude variations of the 100 kyr cycle, both records (coccoliths and wet-bulk density) were filtered with a band pass filter centered on 1/111 kyr^{-1}, with cutting frequencies of 1/90 and 1/140 kyr^{-1}, and after interpolation of the two records at a constant time interval of 20 kyr (in the case of the density record all the measurements belonging to a 20 kyr interval were averaged). It is apparent that the 100 kyr cycle physically exist in the records (Figure 9) and that the filters respond even to relatively small amplitude variations. It is also clear that higher amplitudes of the 100 kyr cycle in the filtered records correspond also to higher variations in the original records. The 100 kyr cycles are in phase in the two records (or with a small non significant lag) (Figure 9c) especially when the cycles have high amplitudes, implying that they respond to the same phenomenon (even though the original series do not appear to vary in parallel, at least in the long term).

The envelopes of the filtered series (Figure 10) show that while the long-term variations of the unprocessed data appear to be dissimilar, the envelopes of the filtered series exhibit common features (see below for cross-spectral analysis tests). Although discrepancies in the amplitude of

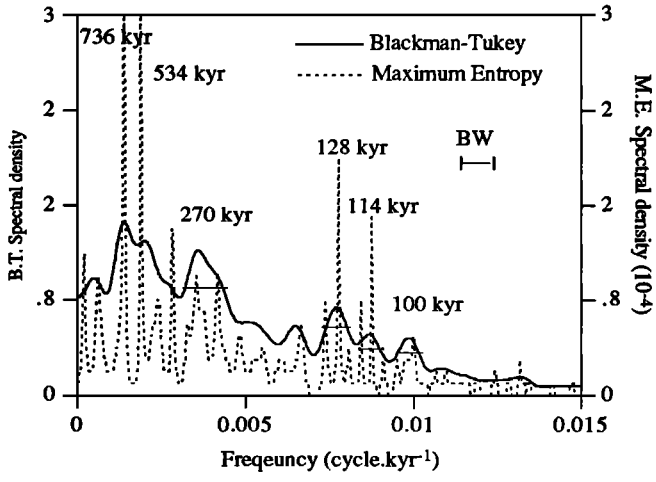

Figure 8. Periodogram of the envelope of the wet-bulk density record filtered with band pass filter centered on 1/20 kyr^{-1}, with cutting frequencies of 1/17 and 1/24 kyr^{-1}. The presence of a peak at 128 and 114 kyr show that the precession cycles recorded in the wet-bulk density record are modulated with period close to 100 kyr cycles as in the Milankovitch theory.

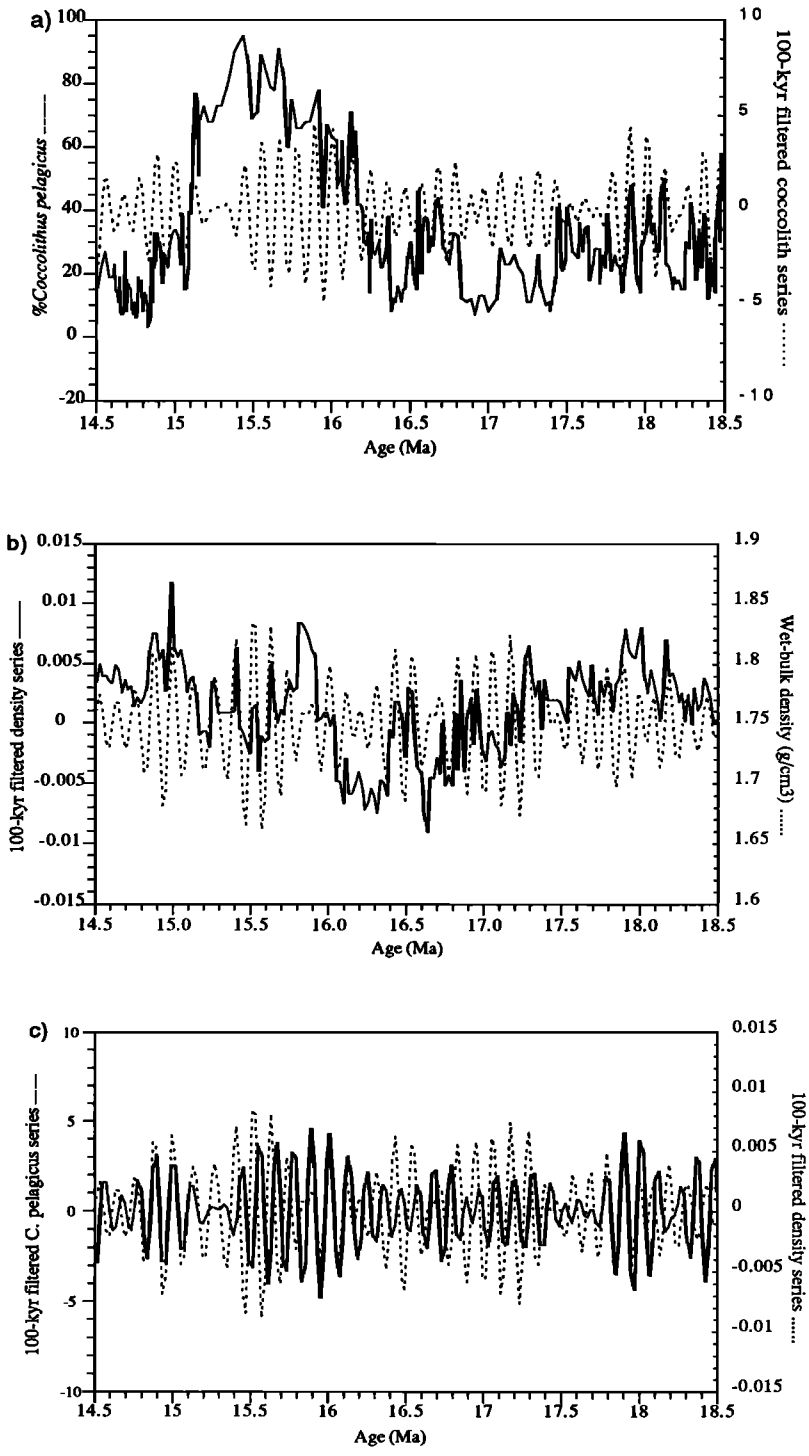

Figure 9. The 100 kyr cycle in the time domain in a four million years long interval: (a) Comparison of the percentage of *C. pelagicus* series and its filtered series with a Gaussian filter centered at 111 kyr cutting at 90 and 140 kyr. Peaks in the raw data generally correspond to peaks in the filtered series, pointing to the relative importance of the 100 kyr cycle.(b) Comparison of the density series (each point correspond to the average of all points contained in 20 kyr intervals) and its filtered series with a Gaussian filter centered at 111 kyr cutting at 90 and 140 kyr. Peaks in the raw data generally correspond to peaks in the filtered series, pointing to the relative importance of the 100 kyr cycle. (c) Comparison of the filtered series of *C. pelagicus* (solid line) and the filtered density series (dotted line). The two series are essentially in phase (especially well marked when the amplitude is high).

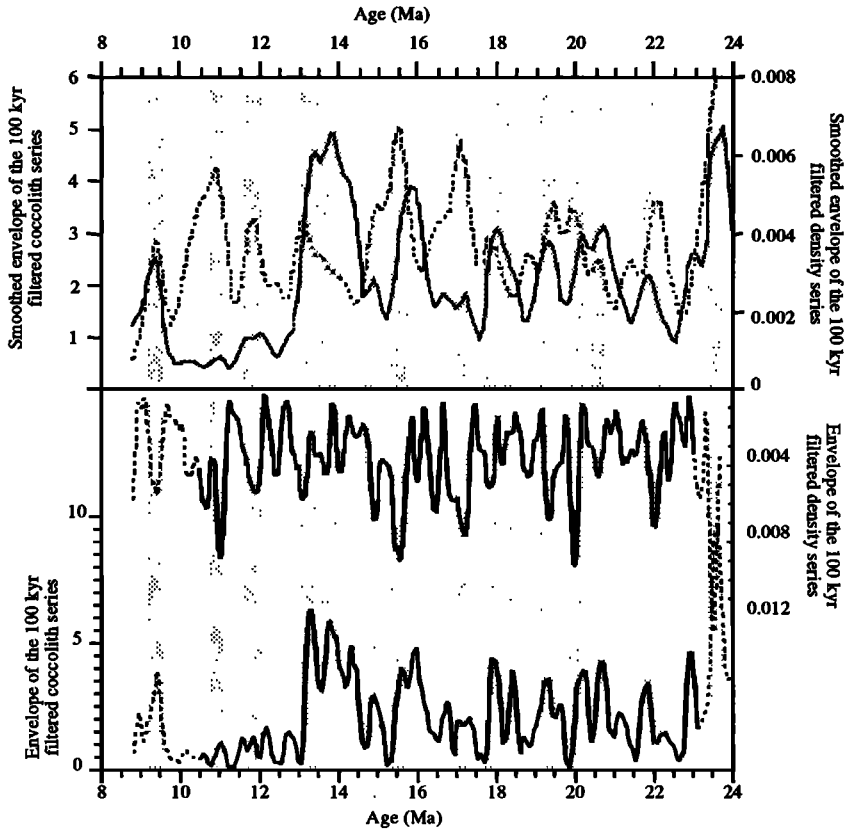

Figure 10. Comparison of the envelope of the 100 kyr filter of the two series : The envelopes of the 111 kyr filter were drawn by connecting the absolute values of the maxima and minima of the filtered series. Intervals of synchronous high amplitude in the two series are shaded. (Lower graph) The dotted parts at the two ends of the curves correspond to lost parts of the filters which were recovered by cyclic convolution. The lower curve is the envelope of the coccolith filter, the upper curve is the envelope of the density filter (revert scale). The curves are mirror images. Equivalent high frequencies (~1 m.y.$^{-1}$) are seen in the two curves. (Upper graph) The smoothed envelopes are here consider for comparison of the longer term similarities. Note that in this uppergraph the density series is not on a revert scale.

some peaks remain, the peaks have the same timing. The amplitude disparities may result from differences in the original data. For example, the *C. pelagicus* values are extremely low between 12.5 and 10 Ma, as are the 100 kyr cycle in this part of this record. In any case the coincidence of the maxima and minima in these two independent records whose raw data yield a different pattern, demonstrate the fact that the 100 kyr cycle varies through time.

The amplitude maxima of the 100 kyr cycle in the filtered *C. pelagicus* series over the intervals 14-13 Ma, 21.5-20 Ma and 24.2-22.8 Ma correlate with intervals of high abundance in *C. pelagicus* and to well-known cooling events revealed by $\delta^{18}O$ records (mid-Miocene-cooling event between 14-12.6 Ma [*Shackleton and Kennett*, 1975; *Vincent and Killingley*, 1985] and Oligocene/Miocene boundary cooling event at 24 Ma [*Miller and Fairbanks*, 1985; *Miller et al.*, 1991]. Amplitude maxima of the 100 kyr cycle correlate with other known high $\delta^{18}O$ values. These variations are global and identified in several Miocene isotopic records from different oceans and are labeled "Mi" [*Miller et al*; 1991]. *Wright et al.* [1992a] identified the Mi events in the benthic foraminifera $\delta^{18}O$ record at Site 747. Oxygen Isotopic Events Mi 1, Mi 1aa, Mi 1b, Mi 2, Mi 3, Mi5, and Mi6 are synchronous with increases of 100 kyr cycle amplitudes (Figure 11): When compared with the relative increase of $\delta^{18}O$ ($\Delta\delta^{18}O$) for each $\delta^{18}O$ peak, it appears that most of $\Delta\delta^{18}O$ peaks (and consequently Mi events) are synchronous of major increases of the 100 kyr cycle amplitude, but Mi 1a and Mi 4 seem not to correspond to increases of the 100 kyr cycle amplitude. With the coarse sample interval of the $\delta^{18}O$ record (~160 kyr), it is not possible to use this record directly for the study of the 100 kyr cycle. Estimated Miocene ice volume, inferred from the $\delta^{18}O$ changes, fluctuated between 60 and 90% of the modern Antarctic ice sheet [Wright et al., 1992b]. All this indicates that during the Miocene the 100 kyr cycle was expressed during time of glacial intensifications, just as they were in the late Pleistocene. However, a major difference exists between the Miocene and the Pleistocene glacial environment that is the presence of large northern hemisphere ice sheet during the Pleistocene. Fluctuations of the size of the large northern hemisphere ice sheets are the driving force of the 100 kyr cycle during the

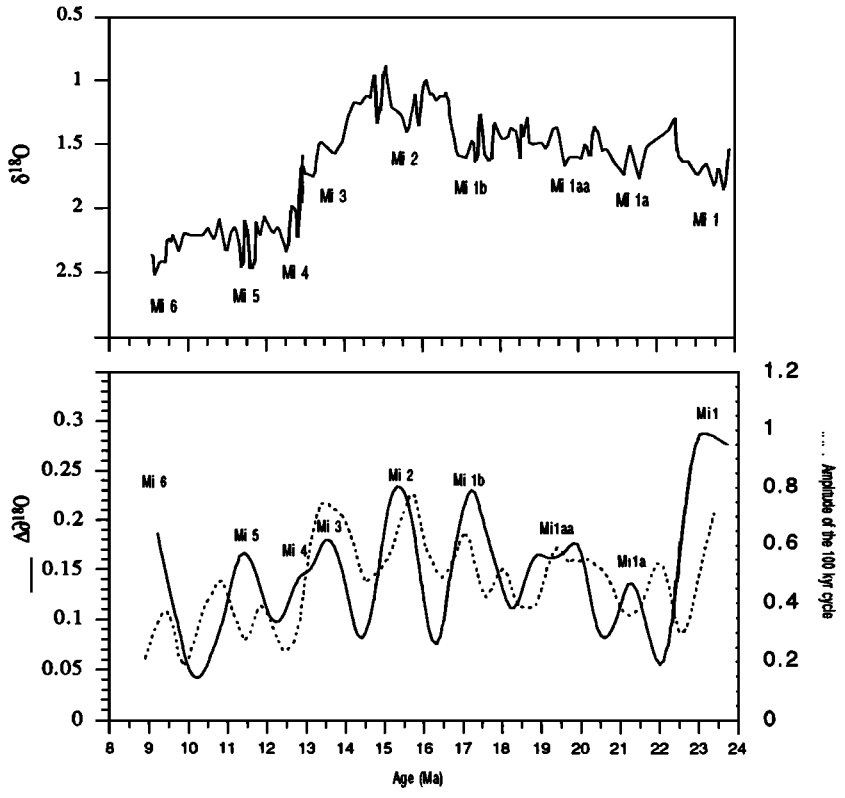

Figure 11. Comparison of the modulation of the 100 kyr cycle and the million year variability of the $\delta^{18}O$ record at ODP Site 747. (Upper) The $\delta^{18}O$ record from benthic foraminifera at site 747 [*Wright et al.*, 1992a]. (Lower) Solid line: smoothed $\Delta\delta^{18}O$ record obtained by subtraction from the $\delta^{18}O$ record of a line going through all the minima of the $\delta^{18}O$ record (before subtraction the series were subsamples with a constant time interval of 50 kyr), dotted line: smoothed and combined 100 kyr envelope (addition of standardized 100 kyr envelopes of the wet-bulk density and the abundance of *C. pelagicus*,). Mi labels are those of *Miller et al.* [1991] identified in the site 747 $\delta^{18}O$ record by *Wright et al.* [1992a]. Correspondence of most of Mi events and high amplitude of the 100 kyr cycle is evident.

Pleistocene [*Imbrie et al.*, 1993]. The southern hemisphere ice sheets should have played the role of their pleistocene northern counterparts, with fluctuations, large enough (60 to 90%) to induce 100 kyr cycles.

Dynamics of the Modulation of the 100 Kyr Cycle

Spectral analysis were performed on the two envelope series (which represent the modulation of the eccentricity cycles in the two series). Frequencies of 2.30, 1.20 and 0.86 m.y.$^{-1}$ are found in the *C. pelagicus* record (Figure 12a) and 2.170, 1.615, 1.164, 0.780 m.y.$^{-1}$ and in the wet-bulk density record (Figure 12b). From cross-spectral analysis of the two series it appears that significant coherency exists at frequencies close to 2.20, 1.30, 0.80, and 0.70 m.y.$^{-1}$. The coherency confirms what I have called above similar features between the two records.

From recent and most accurate obliquity and eccentricity values [*Laskar*, 1988; *Berger and Loutre*, 1991] it is possible to calculate precisely the modulation terms of these parameters. The modulation of the eccentricity calculated from its five most important terms exhibits 10 periods. Eight periods fall between 120 and 500 kyr and two periods equal 2.38 m.y. ($\varepsilon3-\varepsilon5=1/123818-1/130615=\varepsilon2-\varepsilon4=1/94782-1/98715$). Of the 10 periods of the obliquity modulation calculated from its five most important terms, four periods fall between 150 and 190 kyr, three equal 2.38 m.y. ($\varepsilon1-\varepsilon3$ = 1/40392-1/41090= $\varepsilon1-\varepsilon5$ = 1/41090-1/41811 = $\varepsilon2-\varepsilon3$ = 1/39719-1/40392), two equal 1.19 m.y. ($\varepsilon1-\varepsilon2$ = 1/41090-1/39719 = $\varepsilon3-\varepsilon5$ = 1/40392-1/41811) and one equals 0.79 m.y. ($\varepsilon2-\varepsilon5$ = 1/39719-1/41811). It should be noted that surprisingly the long terms of the modulation of the obliquity and the eccentricity are equivalent, a fact that Laskar [1988] finds as a common feature for the inner planets of the solar system and corresponds to a strict resonance in the leading terms of the eccentricity and inclination systems (2E3-2E4 = I3-I4).

The theoretical long-term variations of the Earth's orbital parameters cannot be computed for the interval 10-24 Ma. In order to compare the modulation frequencies found

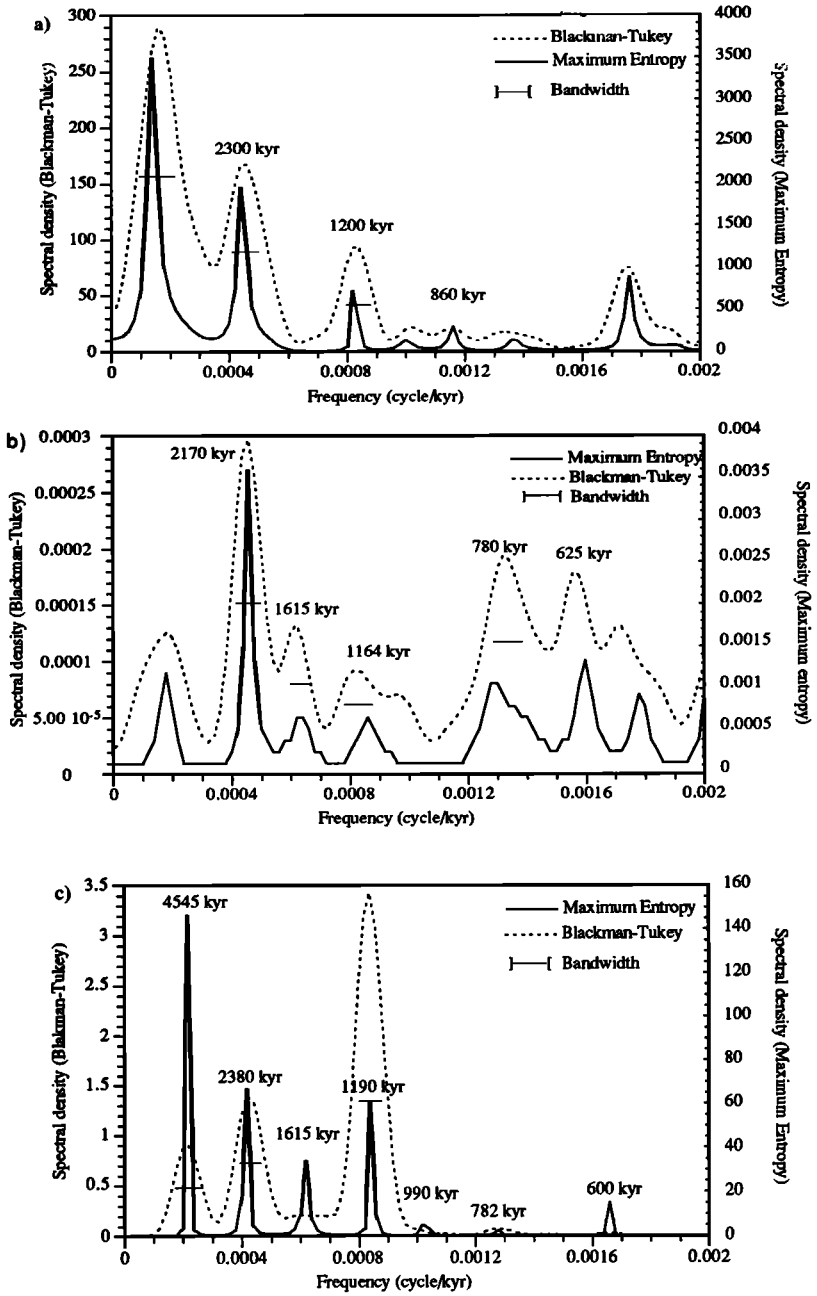

Figure 12. Periodograms (Blackman-Tukey: solid line; and maximum entropy: dotted line) of the modulation series. (a) Analysis of the modulation of the 100 kyr cycle in the *C. pelagicus* series. (b) Analysis of the modulation of the 100 kyr cycle in the density series.(c) Analysis of the modulation of the obliquity.

in the Miocene with theoretical frequencies, the envelope (absolute value of minima and maxima of a curve) of the obliquity for the last 4.76 Ma is taken from the estimation of *Berger and Loutre* [1991] and replicated down to 24 Ma. A duration of the 4.76 m.y. is chosen because it corresponds to the smallest common multiple of the major modulating frequencies of the obliquity (i.e. 4.76=2x2.38=4x1.19=6x.79). Also, since these long-term frequencies are expected to be stable for a time longer than 24 Ma, the record is assumed to be reiterated identically every 4.76 m.y.. Spectral analysis were performed after interpolation with a 20 kyr spacing. The major modulating frequencies are found as expected (Figure 12c). Cross-spectral analysis between the two records from ODP site 747 shows high coherencies at these frequencies, implying a link between the series (Figure 13).

In the three envelope series (coccoliths, density, and obliquity), the 1190 and 800 kyr cycles are in phase (shaded area in the coherency figures). A physical link exists therefore between the series at these frequencies. The

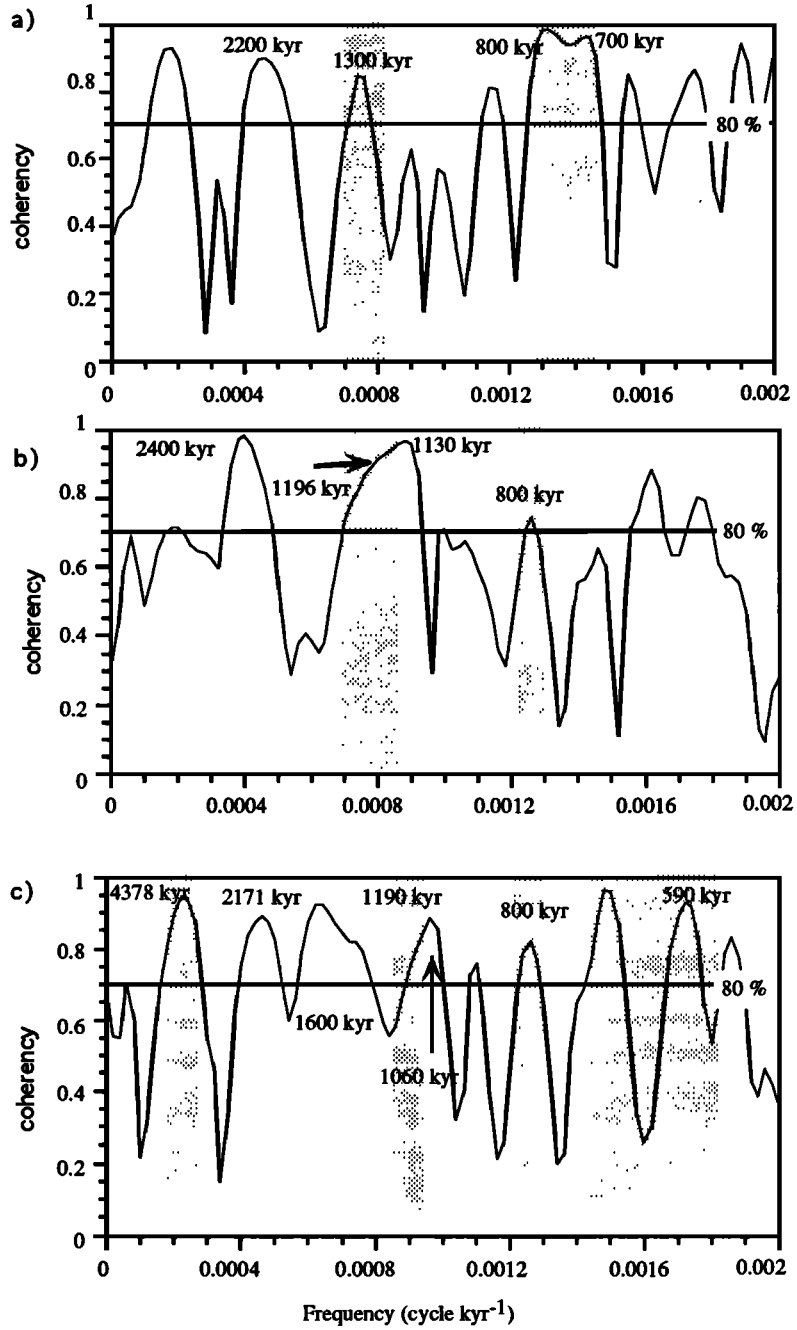

Figure 13. Cross spectral analysis (Blackman-Tukey) of the envelope series: the horizontal line represents the 80% confidence interval level; and the shaded area indicates the frequencies at which the phase is close to zero. (a) Analysis of *C. pelagicus* versus the density envelope series. (b) Analysis of *C. pelagicus* versus the obliquity envelope series. (c) Analysis of density versus obliquity envelope series.

2380 kyr cycles are out of phase. Therefore the response is nonlinear at this frequency. An explanation to this may be found in the fact that the 800 kyr cycle is weak in the envelope of the obliquity and stronger in the envelopes of the coccolith and density series (this strong 800 kyr cycle can result from enhancement of the 400 kyr cycle). The combination of the 800 and the 1190 kyr cycles give rise also to a 2380 kyr cycle. Therefore the original 2380 kyr cycle may shift in phase due to difference in the strength of the 800 kyr cycle. In Figure 14 the three envelopes were filtered at the three frequencies (2.38, 1.19, and 0.79 m.y.). The resulting filters were added in each series, in order to reconstruct the ideal variations with these three components only. For the envelope of the obliquity the 800 kyr filter is multiplied arbitrarily by 10 before the computation. In doing so, it is observed (Figure 14a) that the 2300

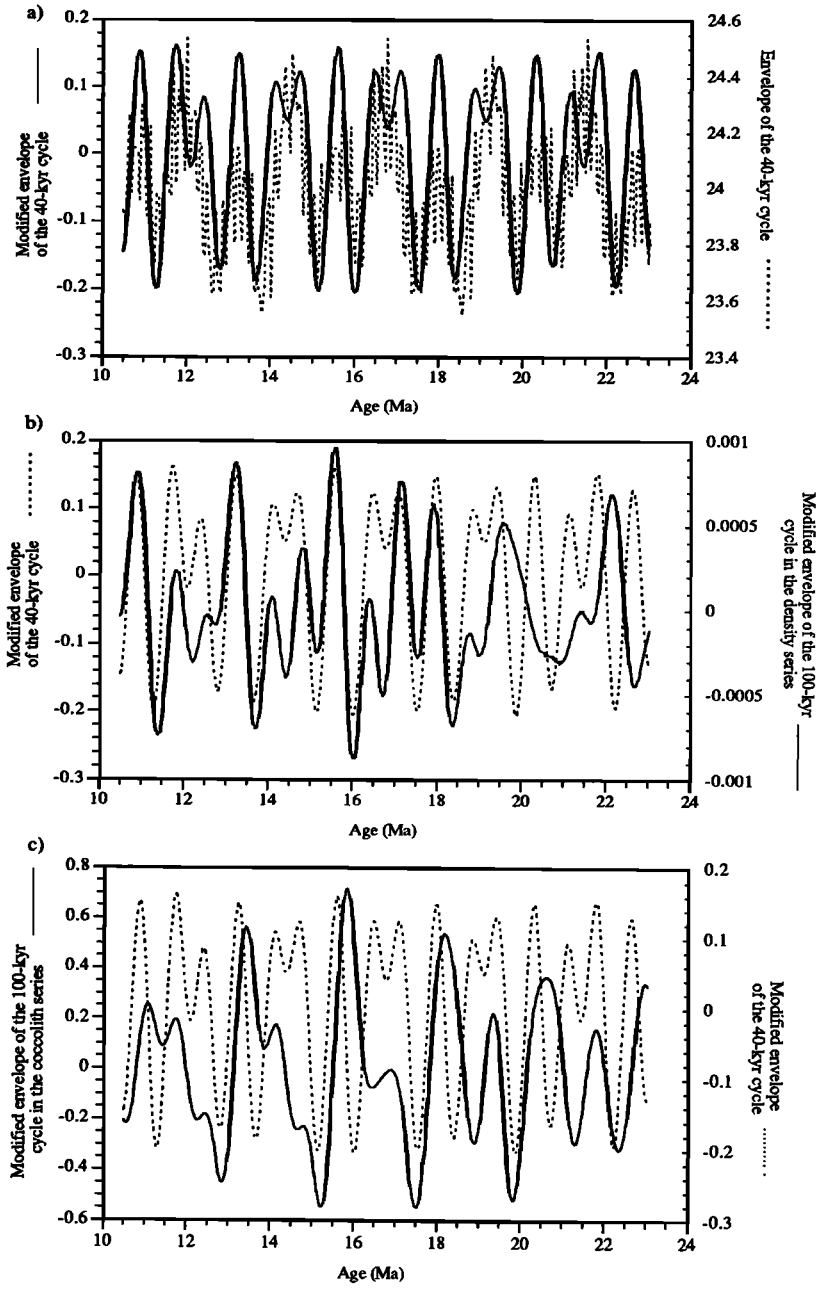

Figure 14. Comparison of the combined terms of the obliquity modulating system in the different series. The envelope of each series is filtered at 2.38, 1.19, and 0.79 m.y. and for each series the three filtered series are added together. In the case of the obliquity the envelope of the 0.8 m.y. filter was multiplied by 10 before addition in order to enhance this signal. (a) Comparison of the unprocessed envelope of the obliquity system with the transformed obliquity envelope. (b) comparison of the filtered density envelope versus the filtered and transformed obliquity envelope. (c) Comparison of the filtered coccolith envelope versus the filtered and transformed obliquity envelope.

kyr cycles have been shifted from the original envelope of the obliquity, and a good match exists between the three resulting series (Figures 14b and 14c). Another possibility for coherency without phase at 2380 kyr period, could result from the fact that the obliquity and the eccentricity systems have both a modulating period of 2380 kyr not in phase with each other.

Interpretations

The periods of the modulation of the 100 kyr cycle recorded in ODP Site 747 sediments are equivalent to the predicted values, suggesting a forcing from one of the two systems (obliquity or eccentricity) or from the two combined.

1. A control of the eccentricity is the most natural explanation: an increase of the eccentricity would result in larger 100 kyr cycles recorded in the sediment. However, this hypothesis is not without problems. Most of the power of the modulation of the eccentricity cycle is concentrated between 120 and 500 kyr, so that the modulation forcing of the 2.38 m.y. cycle is not strong. Also, during the last million year the amplitude of the eccentricity was generally lower than between 1 and 2 Ma [*Berger and Loutre*, 1991, Figures 4a and 5a]. Thus, the appearance of 100 kyr cycle in the late Pleistocene may not be explained by an increase of the amplitude of the eccentricity (but this does not mean that this is not true for the Miocene). Finally, periods of 1.19 and 0.79 m.y. are not evident in the eccentricity modulation system (but they are harmonics of 2.38 m.y.). Thus the presence of strong 403 kyr cycles which are eccentricity related, at ODP Site 747, argues in favor of a scenario in which the eccentricity plays a significant role.

2. The comparison of the recorded 100 kyr modulation with the obliquity system is particularly promising. The obliquity modulation is especially pronounced on the long term frequency band and yields three major periods. They are all found in the 100 kyr modulation spectrum of the Site 747 series. A good correlation exists between the different modulation curves, especially between the *C. pelagicus* record and the theoretical obliquity curves (Figure 14). Cross-spectral analysis shows significant coherency of the two sedimentary series with the obliquity for the modulating periods (Figure 13).

This explanation is also supported by the fact that the amplitude of the obliquity cycle has increased since 0.8 Ma [*Berger and Loutre*, 1991, Figure 4b] correlatively to the amplitude of the 100 kyr cycle recorded by paleoclimatic markers [*Pisias and Moore*, 1981; *Ruddiman et al.*, 1986, 1989].

Another piece of evidence that shows the importance of the modulation of the obliquity system is the existence of 160 to 200 kyr cycles in several paleoclimatic series (*Herbert and Fischer* [1986], *Briskin and Harrell* [1980], *Tiwary* [1987], among others, including this paper's series shown in Figures 4,5, and 6) from which 100 kyr cycle were also recorded. Liu [1992] found also a 185 kyr cycle in the asymmetry of the obliquity cycle. The modulation of the obliquity cycles may explain the presence of these 200 kyr cycles because four of the 10 most important terms of the modulation of the obliquity fall into this range of frequency, 175 kyr being the major one.

An obliquity related modulation of the 100 kyr cycle may be explained theoretically in two different ways. (1) The first is direct (astronomic) and is related to the new theory of *Liu* [1992], who has recently shown that an asymmetry in the 41 kyr cycle gives rise to a 100 kyr cycle, which would have a significant effect on the decay and growth of ice sheets. In this case, the 100 kyr cycle would be directly modulated by the periods specific to the obliquity system (to which this 100 kyr cycle belongs). However, the clear link existing between precession and eccentricity observed in the wet-bulk density record, in the absence of a strong obliquity signal does not support this hypothesis. (2) The second is indirect (climatic). The forcing of the obliquity on climate has a stronger effect at high latitudes where ice sheets form. An increase of the amplitude of the obliquity cycle would favor a long-term increase of ice-sheets: *Pisias et al.* [1990] speculated on an obliquity-linked mechanism enhancing the ice growth. With larger ice-sheets the nonlinear response of climate on the 100 kyr^{-1} frequency band [*Imbrie and Imbrie*, 1980; *Imbrie et al.*, 1993] would be increased.

3. It is also possible that the obliquity and eccentricity systems act together in the modulation of the 100 kyr cycle. The 2.38 m.y. cycle exists in both systems and the 0.79 m.y. cycle is very close to 2x403 kyr.

4. Whatever the modulation mechanism is, internal processes such as tectonic uplift and change of topography of the global ocean (e.g. opening of the Panama Isthmus [*Keigwin*, 1978]) which are not cyclic events, could have more dramatic effects on climate and therefore on the 100 kyr cycle than the modulation. The best evidence for that is the fact that the 100 kyr cycle is stronger during the Pleistocene than at any other time in the Neogene. The modulation could force the timing of the response to such a strong event. In addition, the forcing of the modulation would be climatically important in the absence of a pronounced event.

Conclusions

The main conclusion of this study include the following:

1. The presence of the 100 kyr cycle in the climatic record is not a feature specific of the late Pleistocene. It is not possible with the two records presented here, to compare the magnitude of the amplitude of the 100 kyr cycle from the Pleistocene and the Miocene, although it is probable that the imprint of these cycles was weaker during the Miocene. As for the late Pleistocene, the Miocene 100 kyr cycle has stronger amplitudes during glacial time as inferred from $\delta^{18}O$ records (Mi events of *Miller et al.*, [1991]). It is therefore suspected that the 100 cycle and the MI events have a common origin. Theories which account for the 100 kyr strength in the Pleistocene [e.g., *Imbrie and Imbrie*, 1980; *Saltzman*, 1987; *Liu*, 1992] are also tenable for the Miocene. However, during the Miocene the 100 kyr cycle would have been related to fluctuations of the southern hemisphere ice sheets.

2. The 100 kyr cycle appears episodically on a million year scale. The uplift theory of glacial intensification [*Ruddiman et al.*, 1986; *Raymo et al.*, 1989] cannot account for fluctuations on such short scales but could account for longer-term glacial increases. Modeling by *Saltzman and Maasch* [1990, 1991] and *Saltzman and Verbitsky* [1992] shows that a decreasing mean level of atmospheric CO_2 would result in the appearance of the 100 kyr cycle in the late Pleistocene. This atmospheric CO_2 lowering was seen as a possible "result of rapidly uplifted topography" [*Saltzman and Maasch*, 1991, p. 324], if so, the dynamics of the uplift must be more

episodic than regular to account for the recurrent 100 kyr episodes observed here.

3. The amplitude of 100 kyr cycle varies quasi-periodically with frequencies equivalent to those of the modulation of the orbital parameters (obliquity and eccentricity). Unless it responds to orbital forcing, tectonics alone cannot be the leading factor of climatic variations on the million year scale. The modulation of orbital parameters may act as a catalyzer for climates: when the amplitude of the obliquity and/or the eccentricity cycles exceeds a given threshold, the chances of glacial initiation are increased. These long-term variations in the orbital system are superimposed on the effect of other important phenomena such as tectonics (e.g., Asian uplift), and act in synergy with it, thus regulating the timing of the occurrence of long term climatic effects. Therefore the study of the modulation of the 100 kyr cycle should open new horizons on the dating and the understanding of climate changes on the order of the million years scale.

Acknowledgments. I thank J. Imbrie for helpful discussions and suggestions and M.-P. Aubry for her constant support and discussions. Reviews by M.-P. Aubry, F. Bassinot, W.A Berggren, S. D'Hont, T. D. Herbert, Y. Lancelot, J. G. Ogg, J. Park, E. Vincent, and an anonymous reviewer greatly improved early draft manuscript. This work was supported by the INSU-DBT Thème II program (LGQ contribution N° 95001).

References

Beaufort, L., Dynamique du nannoplancton calcaire au cours du Néogène, *Doc. Lab. Geol. Lyon, 121*, pp. 141, 1992.

Beaufort, L., and M.-P. Aubry, Paleoceanographic implications of a 17-M.Y. long record of high-latitude Miocene calcareous nannoplankton fluctuations, *Proc. Ocean Drilling Program Sci. Results, 120*, 539-549, 1992.

Beaufort, L., and M.-P. Aubry, Fluctuations in the composition of late Miocene calcareous nannofossil assemblages as a response to orbital forcing, *Paleoceanography, 5*, 845-865, 1990.

Berger, A. and M.F. Loutre, Insolation values for the climate of the last 10 million years, *Quat. Sci. Rev., 10*, 297-317, 1991.

Berggren, W.A., D.V. Kent, and J.A. Van Couvering, Neogene geochronology and chronostratigraphy, in The chronology of the geological record, edited by N.J. Snelling, *Geol. Soc. London Spec. Pap. 10*, 1985.

Braarud, T., The temperature range of the non-motile stage of *Coccolithus pelagicus* in the North Atlantic region, *Br. Phycol. J., 14*, 349-352, 1979.

Briskin, M. and J. Harrell, Time-series analysis of the Pleistocene deep-sea paleoclimatic record, *Mar. Geol., 36*, 1-22, 1980.

Cande, S.C. and D.V. Kent, A new geomagnetic polarity timescale for the late Cretaceous and Cenozoic, *J. Geophys. Res., 97*, 13.917-13.952, 1992.

Haq, B.U., Biogeographic history of Miocene calcareous nannoplankton and paleoceanography of the Atlantic ocean, *Micropaleontology, 26*, 414-443, 1980.

Hays, J.D., J. Imbrie, and N.J. Shackleton, Variations in the Earth's orbit: Pacemaker of the ice ages, *Science, 194*, 1121-1132, 1976a.

Hays, J.D., J.A. Lozano, N. Shackleton, and G. Irving, Reconstruction of the Atlantic and Western Indian sectors of the 18,000 B.P. Antarctic Oceans, in Investigations of the Late Quaternary Paleoceanography and Paleoclimatology, edited by R. M. Cline and J.D. Hays, *Geol. Soc. Am. Mem.*, 145, 337-372, 1976b.

Heider, F., B. Leidner, and H. Inokuchi, High southern latitude magnetostratigraphy and rock magnetic properties of sediments from sites 747, 749 and 751, *Proc. Ocean Drill. Program, Sci. Res., 120*, 225-245, 1992.

Herbert, T.D., and A.G. Fischer, Milankovitch climatic origin of mid-Cretaceous black shale rhythms in central Italy, *Nature, 321*, 739-743, 1986.

Herbert, T.D., and L.A. Mayer, Long climatic time series from sediment physical property measurements, *J. Sediment. Pet., 61*, 1089-1108, 1991.

Howard, W.R., Carbonate sedimentation during the Miocene and Pliocene on the Southern Kerguelen Plateau (site 751), *Proc. Ocean Drill. Program Sci. Res., 120*, 1073-1077, 1992.

Howard, W.R., and W.L. Prell, Late Quaternary surface circulation of the southern Indian Ocean and its relationship to orbital variations, *Paleoceanography, 7*, 79-118, 1992.

Imbrie, J. and J.Z. Imbrie, Modeling the climate response to orbital variations, *Science, 207*, 943-953, 1980.

Imbrie, J., A. Berger, E.A. Boyle, S.C. Clemens, A. Duffy, W.R. Howard, G. Kukla, J. Kutzbach, D.G. Martison, A. McIntyre, A.C. Mix, B. Molfino, J.J. Morley, L.C. Peterson, N.G. Pisias, W.L. Prell, M.E. Raymo, N.J. Shackleton, and J.R. Toggweiler, On the structure and origin of major glaciation cycles, 2, The 100,000 -year cycle, *Paleoceanography, 8*, 699-736, 1993.

Jenkins, G.M., and D.G. Watts, *Spectral Analysis and Its Applications*, 525 pp., Holden-Day, San Francisco, Calif., 1968.

Keigwin, L.D., Pliocene closing of the Isthmus of Panama, based on biostratigraphic evidence from nearby Pacific Ocean and Caribbean Sea cores, *Geology, 6*, 630-634, 1978.

Laskar, J., Secular evolution of the solar system over 10 million years, *Astron. Astrophys., 198*, 341-362, 1988.

Liu, H.-S., Frequency variations of the Earth's obliquity and the 100-kyr ice-age cycles, *Nature, 358*, 397-399, 1992.

McIntyre, A., Coccoliths as paleoclimatic indicators of Pleistocene glaciation, *Science, 158*, 1314-1317, 1967.

Miller, K.G., and R.G. Fairbanks, Oligocene to Miocene carbon isotope cycles and abyssal circulation changes, in *The Carbon Cycle and Atmospheric CO_2: Natural Variations Archean to Present, Geophys.Monogr. Ser.* Vol. 32, edited by E.T. Sundquist and W.S. Broecker, pp. 469-486, AGU, Washington, D.C., 1985.

Miller, K.G., J.D. Wright, and A.N. Brower, Oligocene to Miocene stable isotope stratigraphy and planktonic foraminifer biostratigraphy of the Sierra Leone Rise (DSDP site 366 and ODP site 667), *Proc. Ocean Drill. Program, Sci. Res., 108*, 279-294, 1989.

Miller, K.G., J.D. Wright, and R.G. Fairbanks, Unlocking the icehouse: Oligocene-Miocene oxygen isotope, eustasy and margin erosion, *J. Geophys. Res., 96*, 6829-6848, 1991.

Oelermans, J., Model experiments on the 100,000-yr glacial cycle, *Nature, 287*, 430-432, 1980.

Park, J., and K. Maasch, Plio-Pleistocene time evolution of the 100-kyr cycle in marine paleoclimate records, J. Geophys. Res., 98, 447-461, 1993.

Pisias, N.G., A.C. Mix, and R. Zahn, Nonlinear response in

the global climate system : evidence from benthic oxygen isotpic record in core RC13-110, *Paleoceanography, 5*, 147-160, 1990.

Pisias, N.G. and T.C.J. Moore, The evolution of the Pleistocene climate: A time series approach, *Earth Planet. Sci. Lett., 52*, 450-458, 1981.

Pollard, D., Ice-age simulations with a calving ice-sheet model, *Quat. Res., 20*, 30-48, 1983.

Press, W.H., B.P. Flannery, S.A. Teukolsky,.and W.T. Vetterling, *Numerical Recipes*, 818 pp., Cambridge University Press, New York, 1986

Rack, F.R. and A. Palmer-Julson, Sediment microfabric and physical properties record of late Neogene polar front migration, Site 751, *Proc. Ocean Drill. Program, Sci. Res., 120*, 179-205, 1992a.

Raymo, M.E., W.F. Ruddiman, J. Backman, B.M. Clement, and D.G. Martinson, Late Pliocene variation in northern hemisphere ice sheets and North Atlantic deep Water circulation, *Paleoceanography, 4*, 413-446, 1989.

Ruddiman, W.F. and M.E. Raymo, Northern hemisphere climate regimes during the past 3 Ma : Possible tectonic connection, in *The Past Three Million Years: Evolution of Climatic variability in the North Atlantic Region*, edited by N.J. Shackleton, R.G. West, and D.Q. Bowen, pp. 1-20, Cambridge University Press, Cambridge, 1988.

Ruddiman, W.F., M. Raymo, D.G. Martinson, B.M. Clement, and J. Backman, Pleistocene evolution: Northern hemisphere ice sheets and North Atlantic ocean, *Paleoceanography, 4*, 353-412, 1989.

Ruddiman, W.F., M. Raymo, and A. McIntyre, Matuyama 41,000-year cycles: North Atlantic Ocean and Northern hemisphere ice sheets, *Earth Planet. Sci. Lett., 80*, 117-129, 1986.

Saltzman, B., Carbon dioxide and the $\delta^{18}O$ record of late Quaternary climatic change: A global model, *Clim. Dyn., 1*, 77-85, 1987.

Saltzman, B. and K.A. Maasch, A first-order global model of late Cenozoic climate, *Trans. Roy. Soc. Edinburgh, 81*, 315-325, 1990.

Saltzman, B. and K.A. Maasch, A first-order global model of late Cenozoic climate, II, Further analysis based on a simplification of CO_2 dynamics, *Clim. Dyn.*, 5, 201-210, 1991.

Saltzman, B. and M.Y. Verbitsky, Asthenospheric ice-load effects in a global dynamical-system model of the Pleistocene climate, *Clim. Dyn., 8*, 1-11, 1992.

Schlich, R. et al., Site 747, *Proc. Ocean Drill. Program, 120*, 1989.

Shackleton, N.J. and J.P. Kennett, Paleotemperature history of the Cenozoic and the initiation of Antarctic glaciation: Oxygen and carbon isotope analyses: DSDP sites 277, 279, and 281, *Initial Rep. Deep Sea Drill. Proj., 29*, 753-755, 1975.

Tiwary, R.K., Higher-order eccentricity cycles of the middle and late Miocene climatic variations, Nature, 327, 219-220, 1987.

Vincent, E. and J.S. Killingley, Oxygen and carbon isotope record for the early and middle Miocene in the central equatorial Pacific (leg 85) and paleoceanographic implications, *Initial Rep. Deep Sea Drill. Proj., 85*, 749-769, 1985.

Wright, J.D., and K.G. Miller, Miocene stable isotope stratigraphy, Site 747, Kerguelen Plateau, *Proc. Ocean Drill. Program, Sci. Results, 120*, 855-866, 1992.

Wright, J.D., K.G. Miller, and R.G. Fairbanks, Early and Middle Miocene stable isotopes: Implications for deepwater circulation and climate, *Paleoceanography, 7*, 357-389, 1992.

L. Beaufort, Laboratoire de Géologie du Quaternaire, CNRS-Luminy, Case 907, 13288 Marseille Cedex 09, France

(Received January 10, 1994; revised August 11, 1994; accepted August 11, 1994.)